Motion compensated local tomography

Alexander Katsevich

Department of Mathematics
University of Central Florida
Orlando, Florida 32816, USA

Introduction

Cardiac and, more generally, dynamic imaging is a very important challenge facing CT. The main difficulty is that the object being scanned changes during data acquisition. In cardiac CT there are two major groups of approaches for dealing with this issue.

Approach 1

One is based on gating, i.e. selecting the CT data which corresponds to a fixed cardiac phase, and then using mostly that data for image reconstruction. See e.g. papers by a group from Philips (P. Koken, M. Grass, C. Bontus, and others), M. Kachelriess, etc.

Approach 2

The second aproach is based on incorporating a motion model into a reconstruction algorithm. See papers by U.v. Stevendaal, C. Blondel, J. Pack, F. Noo, P. Grangeat, and others.

Typically these algorithms are of iterative nature, but some progress has been achieved towards noniterative reconstruction (Taguchi and Kudo 2007, Desbat, Roux, Grangeat 2007).

Local Tomography - overview

In this talk we develop local tomography (LT) for image reconstruction from motion contaminated data. LT was first proposed in E. Vainberg, E. Kazak, V. Kurczaev 1981 and K.T. Smith and F. Keinert 1985.

Local Tomography - overview

The goal of LT is to compute $\mathcal{B}f$, where $\mathcal{B}$ is an operator that enhances singularities of the object f being scanned. In $\mathbb{R}^2$, $\mathcal{B}$ is an elliptic PDO of order one (see papers by A. Faridani, D. Finch, F. Natterer, AK, A. Ramm, and others). The main advantage of LT is that it does not require irradiating the entire cross-section of the patient.

Background

In AK 2006 we investigated LT in the case of a dynamically changing f. The main assumption in AK 2006 is that no information about the change in f is available.

Now we assume that it is known how f moves. While the problem of motion estimation is quite challenging, significant progress has been achieved in this area and good algorithms are available (see e.g. K. Taguchi et. al. 2006).

A few words on motion

To describe the motion we use the framework of continuum mechanics, i.e. we track the location of individual particles of the object f over time. For the purposes of this talk it is assumed that motion is smooth.

Overview of results - 1

We propose a new LT function f_Λ, which is related to f via an operator $\mathcal{B}$: $f_\Lambda = \mathcal{B} f$. Because of motion, $\mathcal{B}$ may fail to be a PDO. We obtain the conditions that guarantee that $\mathcal{B}$ is a PDO. Under these conditions, similarly to the classical LT in $\mathbb{R}^2$, $\mathcal{B}$ is a PDO of order 1.

Overview of results - 2

Computation of f_Λ depends on a weight function Φ. We show that Φ can be chosen in such a way that the operator $\mathcal{B}$ has principal symbol $|\xi|$.

Overview of results - 3

In practice tomographic data are discrete, and derivatives are usually replaced by their mollified analogues. We consider how mollification affects the singularities of the LT function f_Λ. Using this approach we develop an algorithm for finding values of jumps of f using LT.

Source trajectory

Let C be a smooth curve in $\mathbb{R}^2$

$$[0,T] \ni s \to y(s) \in \mathbb{R}^2,\ |\dot{y}(s)| \neq 0, s \in [0,T].$$

C is also called a source trajectory. Usually the source moves along C with constant speed, so we regard s also as time variable.

More on motion

Fix any $s_0 \in [0, T]$ and call it the reference time. Suppose $y = \psi(s, x)$ is the position of the particle at time s, which is located at x at the reference time $s = s_0$. We assume that for each $s \in [0, T]$ the function $\psi(s, x) : \mathbb{R}^2 \to \mathbb{R}^2$ is a diffeomorphism. Physically this means that two distinct points cannot move into the same position. This assumption is quite natural, since cardiac motion is not infinitely compressible.

More on motion

The inverse of ψ is $x = \mu(s, y) : \mathbb{R}^2 \to \mathbb{R}^2$. μ gives the original position x of the particle at the reference time, which is located at y at time s. We assume that both ψ and μ are identity maps outside of some open set U, which contains the support of the object, and $\psi, \mu \in C^\infty([0, T] \times \mathbb{R}^2)$. As usual, we assume that C is at a positive distance from U.

More on motion

Obviously,

$$\mu(s, \psi(s, x)) \equiv x, \ \psi(s, \mu(s, y)) \equiv y.$$

Since matter is conserved, the x-ray density at time s and point y is given by $|\nabla \mu(s, y)| f(\mu(s, y))$.

The first LT function

Fix any $\Phi \in C_0^\infty([0,T] \times \mathbb{R}^2)$ and define the first LT function:

$$f_1(x) := \int_0^T \Phi(s,x) g(s, \beta(\psi(s,x),s)) ds,$$

where

$$\beta(s,y) := \frac{y - y(s)}{|y - y(s)|}.$$

The first LT function

and g is the data

$$g(s,\beta) := \int_0^\infty |\nabla \mu(s, y(s) + t\beta)| \times f(\mu(s, y(s) + t\beta))dt.$$

The first LT function

Then

$$f_1(x) = \frac{1}{(2\pi)^2} \int_{\mathbb{R}^2} \tilde{f}(\xi) a(x,\xi) e^{-i\xi\cdot x} d\xi,$$

where

$$a(x,\xi) := \int_0^T \int_0^\infty e^{-i\xi\cdot\eta(x,s,t)}(\cdot) dt ds,$$
$$\eta(x,s,t) := \mu(s, y(s) + t(\psi(s,x) - y(s))) - x.$$

The first LT function

Our goal is to show that $f \to f_1$ is an elliptic PDO. Fix $x \in U$ and consider the curve

$$\gamma_s(t) := \mu(s, y(s) + t(\psi(s, x) - y(s))), \ t > 0,$$

for some s. Obviously, $\gamma_s(t)$ is the preimage of the ray

$$L(s, x) := \{y = y(s) + t(\psi(s, x) - y(s)), \ t > 0\},$$

at the reference time $s = s_0$. $\gamma_s(t)$ passes through x when $t = 1$ for any $s \in [0, T]$.

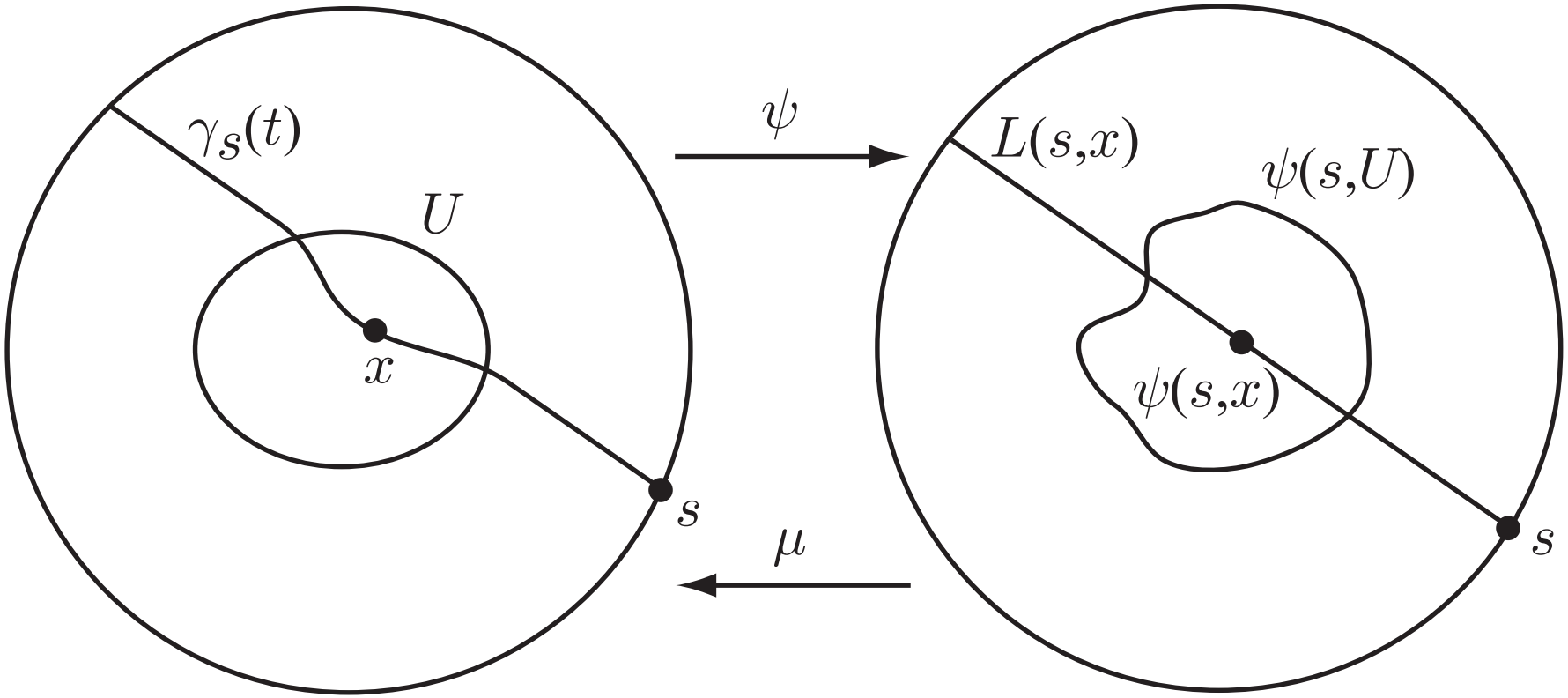
$\gamma_s(t)$
U
x
s
ψ
μ
$L(s,x)$
$\psi(s,U)$
$\psi(s,x)$
s

The first LT function

Denote

$$A(s,x) := \left.\frac{d}{dt}\gamma_s(t)\right|_{t=1}$$
$$= \nabla\mu(s,\psi(s,x))(\psi(s,x) - y(s)).$$

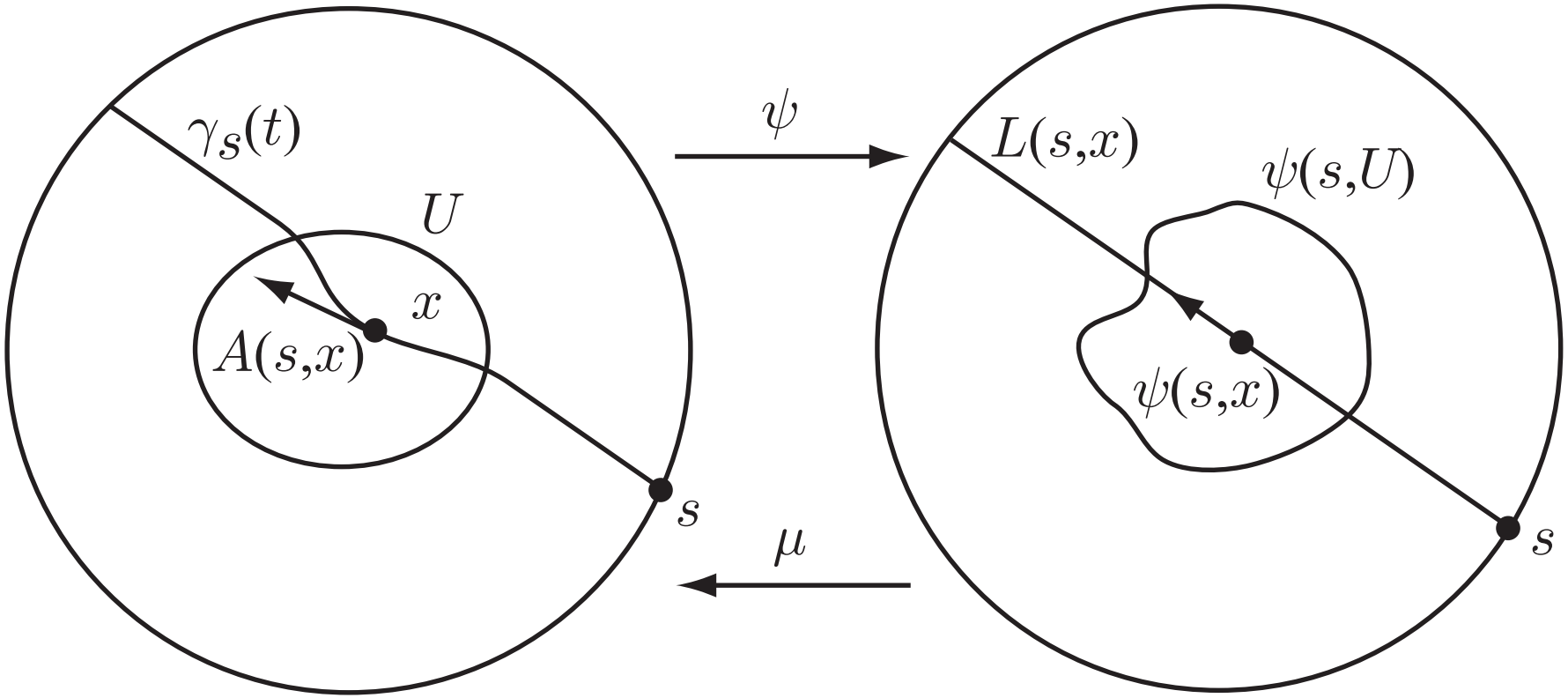
$\gamma_s(t)$
U
x
$A(s,x)$
s
ψ
μ
$L(s,x)$
$\psi(s,U)$
$\psi(s,x)$
s

The first LT function

Fix $\Theta(\theta) = (\cos\theta, \sin\theta)$ and consider the equation

$$\Theta \cdot A(s, x) = 0,$$

which is to be solved for s. Let $s_j = s_j(x, \theta)$, $j = 1, 2, \ldots$, be the solutions. Our main assumption is that at least one locally smooth solution exists for all $x \in U$ and $\theta \in [0, \pi)$. Clearly, a solution s_j is locally smooth if $A(s_j, x)$ and $A'_s(s_j, x)$ are not parallel.

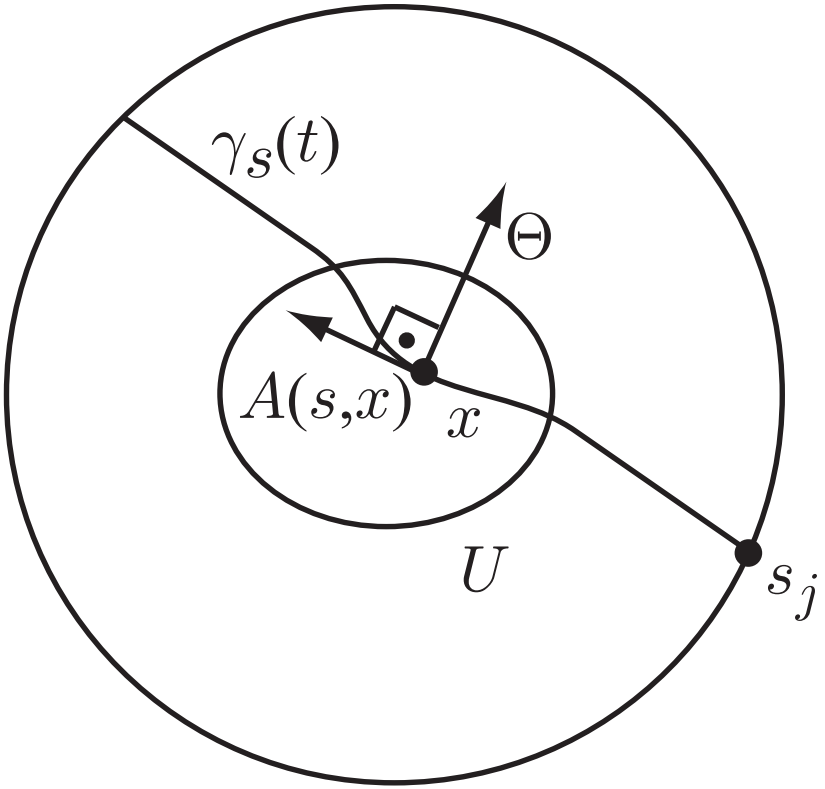
$\gamma_s(t)$
Θ
$A(s,x)$
x
U
s_j

The symbol

The stationary phase method gives

$$a(x, \lambda\Theta_0) =$$

$$\frac{2\pi}{\lambda} \sum_j \frac{\Phi(s_j, x)|s_j'(x, \theta_0)||\nabla\mu(s_j, \psi(s_j, x))|}{|\nabla\mu(s_j, \psi(s_j, x))\beta(s_j, x)|}$$

$$+ O(\lambda^{-2}),\ \lambda \to \infty.$$

Thus a is a symbol from the class S^{-1} microlocally near (x, Θ_0).

The symbol

Choosing Φ appropriately we can get

$$a(x, \lambda\Theta_0) = \frac{2\pi}{\lambda} + O(\lambda^{-2}),\ \lambda \to \infty.$$

Thus f_1 recovers all the singularities of f uniformly, i.e. regardless of their orientation.

Artifacts?

The function f_1 may have additional singularities (artifacts). They may arise if

$$[y'(s)(1-t)+t\psi'_s(s,x)]-\psi'_s(s,\tilde{x}) \parallel \psi(s,x)-y(s)$$

for some $\tilde{x}\in U$, $x\neq\tilde{x}$, such that

$$\tilde{y}:=y(s)(1-t)+t\psi(s,x)=\psi(s,\tilde{x})\in L(s,x).$$

The condition means that there is a particle $\tilde{y}=\psi(s,\tilde{x})$, which instantaneously stays on $L(s,x)$.

Artifacts?

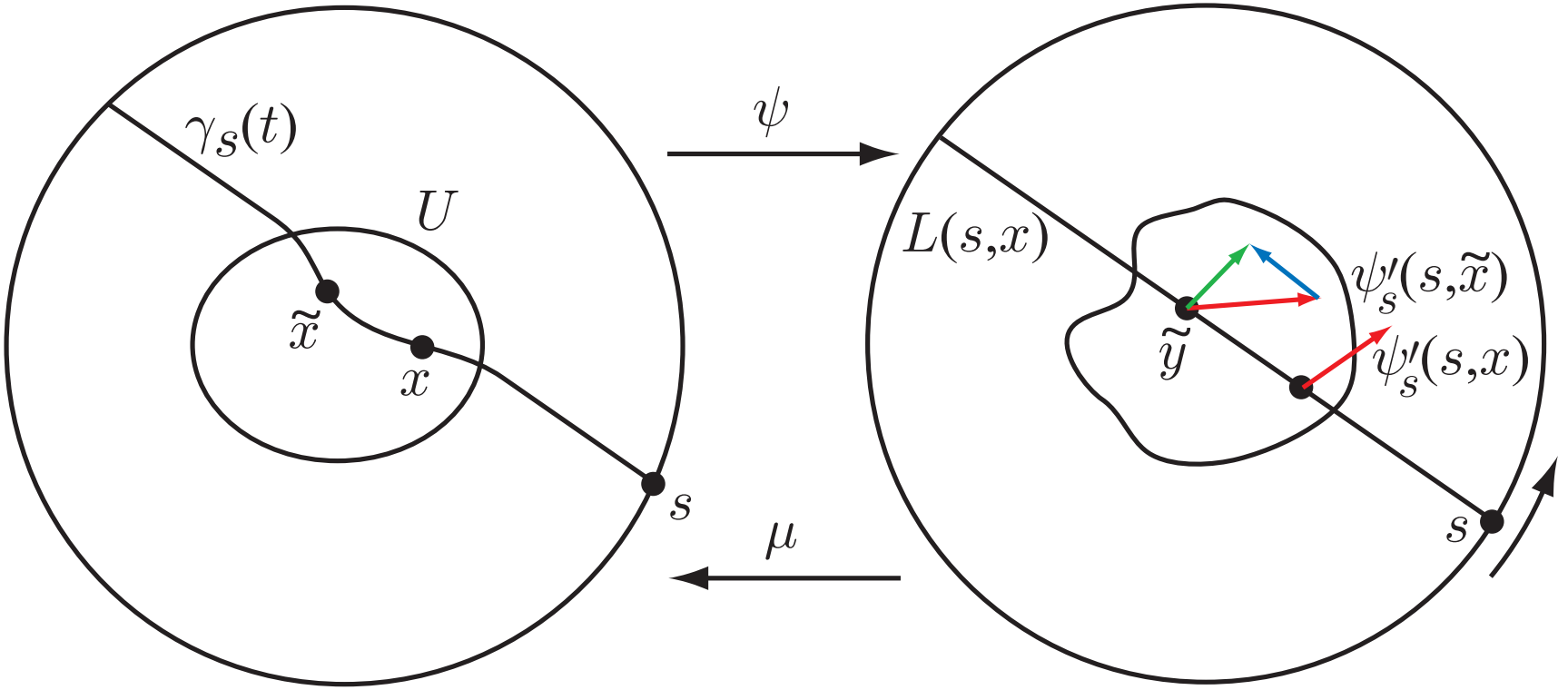

If ψ'_s is sufficiently small and the component of $y'(s)$ perpendicular to $\psi(s,x) - y(s)$ is sufficiently large, then artifacts do not occur.

The second LT function

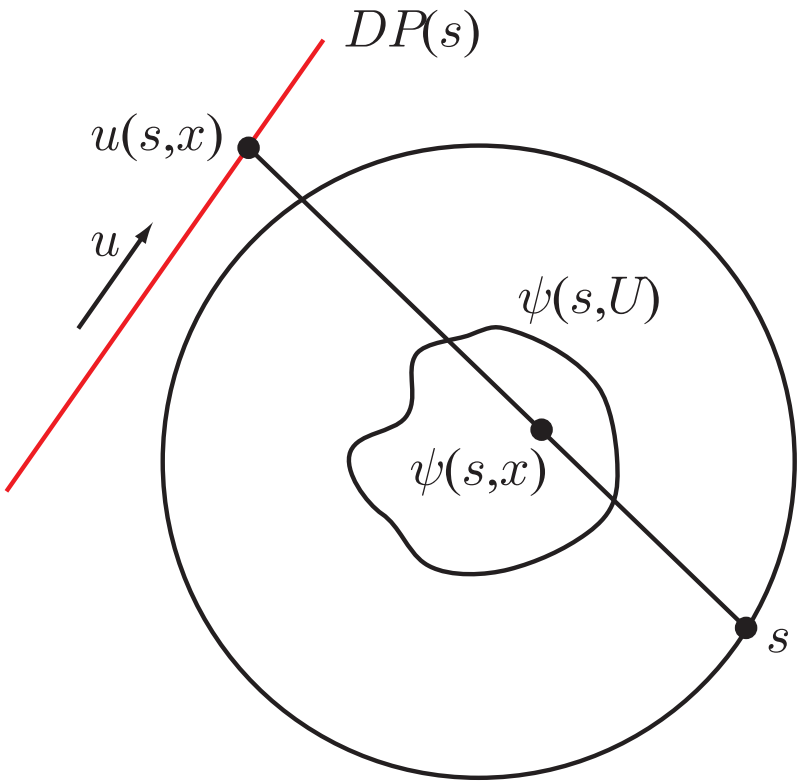

Denote $g(s, \beta(s, x)) = g(s, u(s, x))$.

The second LT function

To emphasize the singularities in f we take the Laplacian of f_1 and retain the leading singular term. This gives the final LT function

$$f_\Lambda(x) := -\frac{1}{2\pi}\int_0^T \Phi(s,x) g''_{uu}(s,u(s,x))ds.$$

Summary

Theorem. Suppose for each $x \in U$ and $\theta \in [0, \pi)$ there exists at least one $s \in (0, T)$ such that

1. $\Theta(\theta) \cdot A(s, x) = 0$, and
2. $A(s, x)$ and $A'_s(s, x)$ are not parallel.

Suppose also that for any $s \in [0, T]$ and $x \in U$ there is no particle $y \in L(s, x)$, $y \neq \psi(s, x)$, which instantaneously stays on the ray. Then $f_\Lambda = \mathcal{B} f$, where $\mathcal{B}$ is a PDO from the class $S_1(U)$ with principal symbol $|\xi|$.

Corollary

Recall the well-known formula:

$$\mathcal{F}^{-1}(1/|\xi|) = 1/(2\pi|x|),\ x, \xi \in \mathbb{R}^2.$$

Fix $\epsilon > 0$, and let $|x|_\epsilon^{-1}$ denote a distribution, which coincides with $1/|x|$ in a neighborhood of $x = 0$, is C^∞ outside of $x = 0$, and equals zero for $|x| > \epsilon$. Define

$$f_{pl}(x) = \frac{1}{2\pi}|x|_\epsilon^{-1} * f_\Lambda(x).$$

Corollary. Under the conditions of the Theorem, the map $f \to f_{pl}$ is a PDO from the class $S_0(U)$ with principal symbol 1.

Corollary

The Corollary implies that the difference $f - f_{pl}$ is smoother than f in the scale of Sobolev spaces. Hence the problem of finding f in the motion contaminated case can be split into two steps. First one finds f_{pl}, which is a high-frequency component of f. At the second step one finds the low-frequency component $f - f_{pl}$ using an iterative approach. The main advantage of this method is that to iteratively find a low-frequency component of an image is much easier than to iteratively find the whole image.

Mollification

For numerical implementation we compute a mollified version

$$f_{\Lambda,\epsilon}(x) :=$$

$$-\frac{1}{2\pi}\int_0^T \Phi(s,x)\int w''_\epsilon(u(s,x)-u)g(s,u)duds,$$

where $w_\epsilon(u)$ is a family of mollifiers. Hence we need to study how $f_{\Lambda,\epsilon}(x)$ reflects the singularities of f.

Mollification

Assume that f is a conormal distribution associated to a smooth surface S. Pick $x_0 \in S$ and assume that supp (f) is contained in a small neighborhood of x_0. Choose a coordinate system such that x_0 is the origin, and S is described by the equation $z_2 = h(z_1)$, where $h(0) = h'(0) = 0$. Thus the z_2-axis is perpendicular to S at x_0.

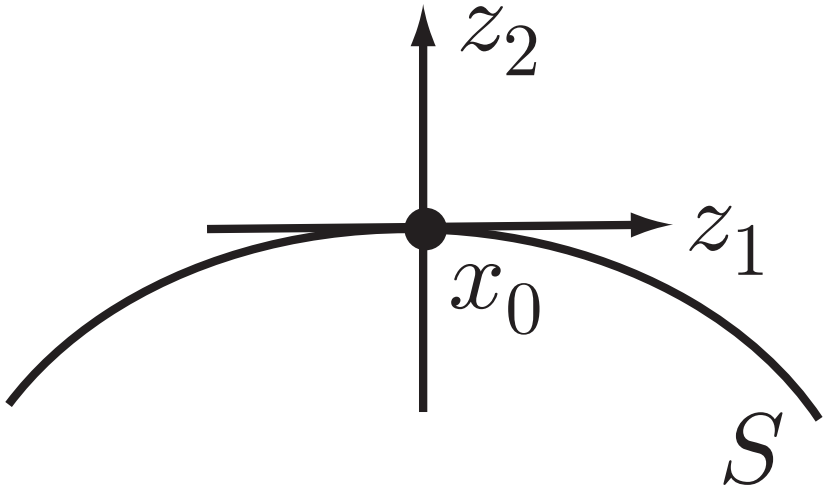

Mollification

Represent the Fourier transform of f in the form

$$\tilde{f}(\xi_1, \xi_2) = \int A(z_1, \xi_2) e^{i(h(z_1)\xi_2 + \xi_1 z_1)} dz_1,$$

where

$$A(z_1, \xi_2) \sim \sum_{k \geq 0} A_k(z_1) \xi_2^{\alpha - k}, \ \xi_2 \to \infty,$$

$A_k(z_1) \in C_0^\infty(\mathbb{R})$ for all $k \geq 0$, the asymptotic expansion can be differentiated with respect to z_1 and ξ_2, and $\alpha \in \mathbb{R}$ is a constant.

Mollification

We show that

$$f_{\Lambda,\epsilon}(x_0 + \epsilon z) = \text{Re}\left\{\int K_\epsilon(z, v) w(v) dv\right\}$$

for some kernel $K_\epsilon(z, v)$.

The nature of the singularity of K_ϵ as $\epsilon \to 0$ depends on the singularity of f across S.

Mollification

The leading singular term of K_ϵ is given by

$$K_\epsilon(z,v) \sim$$

$$\frac{A_0(0)}{\pi\epsilon^{\alpha+2}} \sum_j \Phi(s_j,x_0) \frac{[(e_2\cdot\nabla\mu_j\beta'_u)D(s_j,x_0)]^{-\alpha}}{|\nabla\mu_j\beta(s_j,x_0)\cdot\Theta'_s(s_j,x_0)|}|\nabla\mu_j|$$

$$\times \int_0^\infty \lambda^{\alpha+1}\exp\{-i\lambda(\nabla u(s_j,x_0)\cdot z - v)\}\,d\lambda.$$

We see the dependence on α.

Mollification

Assuming f has a jump discontinuity, we obtain

$$\frac{\partial}{\partial \rho} f_{\Lambda,\epsilon}(x_0 + \epsilon \rho e_2)\Big|_{\rho=0} \sim -D(x_0)\frac{W_0}{\pi\epsilon}, \ \epsilon \to 0,$$

where $W_0 := \int \frac{w(v)}{v^2} dv$.

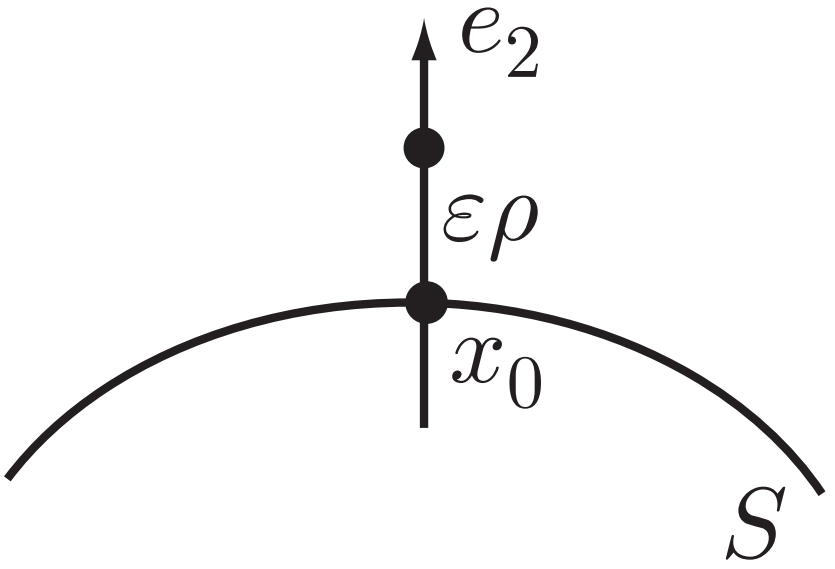

Numerical experiment

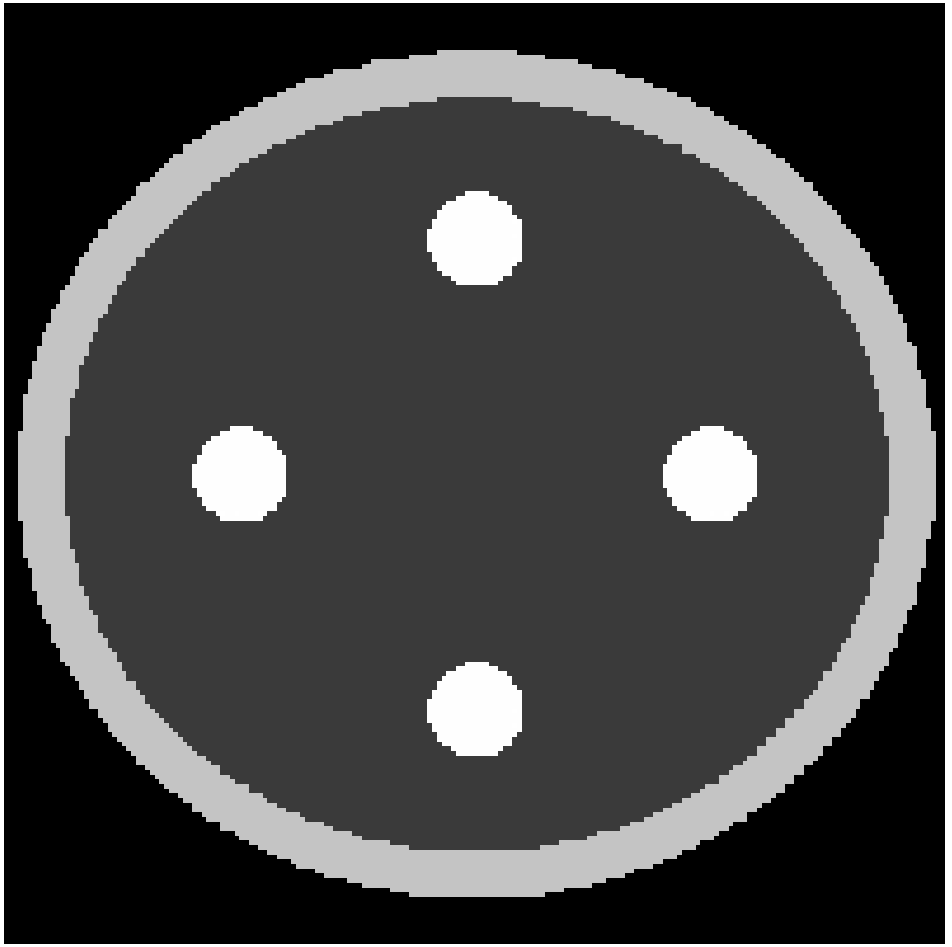

Original phantom at reference time.

Numerical experiment

The motion of the medium is described by the function

$$\psi(s,x) = x + \begin{cases} 15\cos(1.2s)\frac{25-|x-x_0|}{25}(\cos\theta, \sin\theta), & |x-x_0| < 25, \\ 0, & |x-x_0| \geq 25. \end{cases}$$

Here $x_0 = (100, 0)$ is the center around which the motion is taking place and $\theta = 70°$.

Numerical experiment

At reference time the domain $|x_1| < 200, |x_2| < 200$ was split into 500×500 small squares. Then evolution of the grid was tracked over time. It was assumed that each square was mapped into a quadrilateral. To compute the tomographic data we used a ray-tracing algorithm, which was based on computing the lengths of intersections of the rays and quadrilaterals.

Numerical experiment

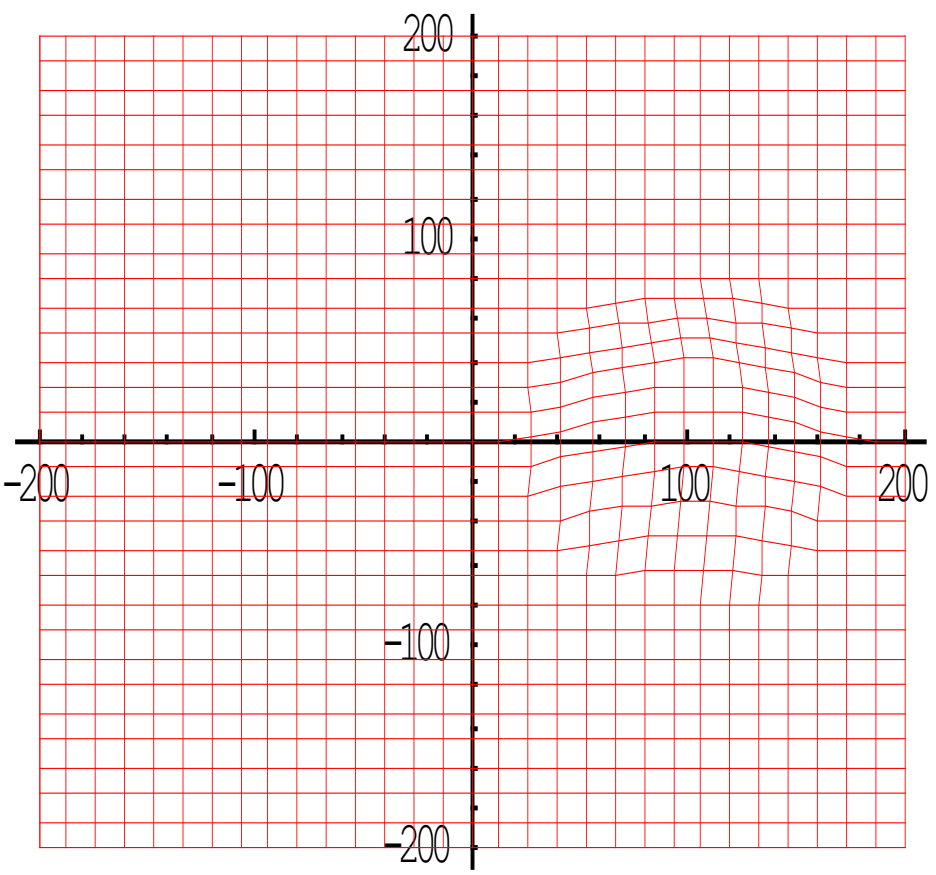

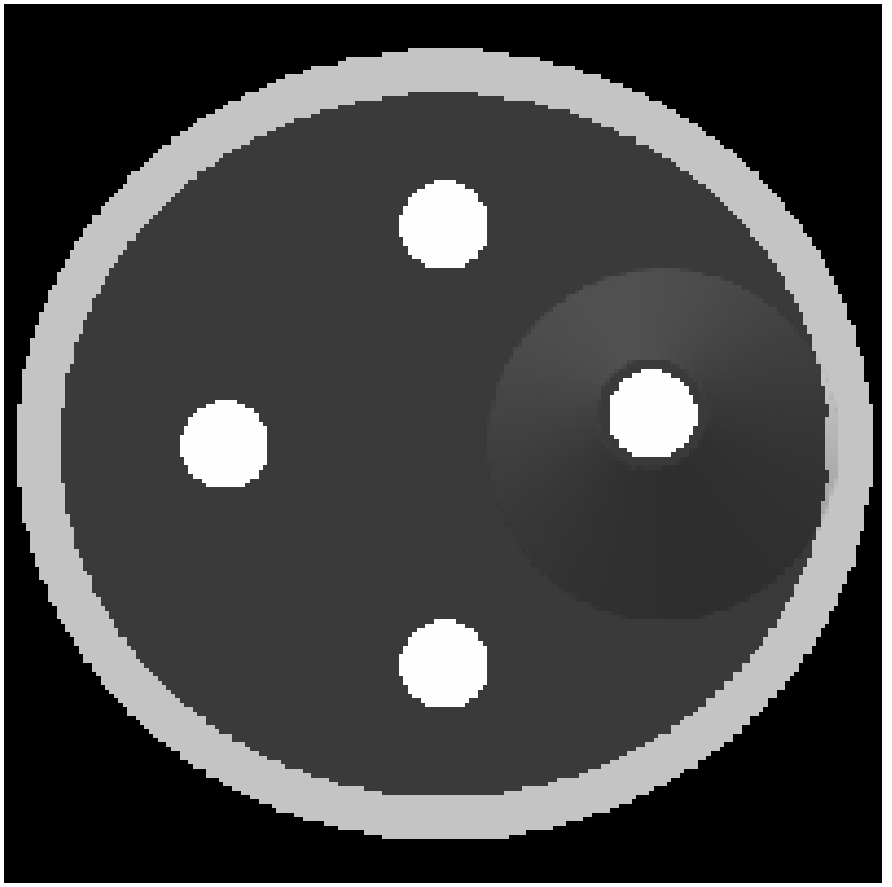

Original image of the phantom at an intermediate time.

Numerical experiment

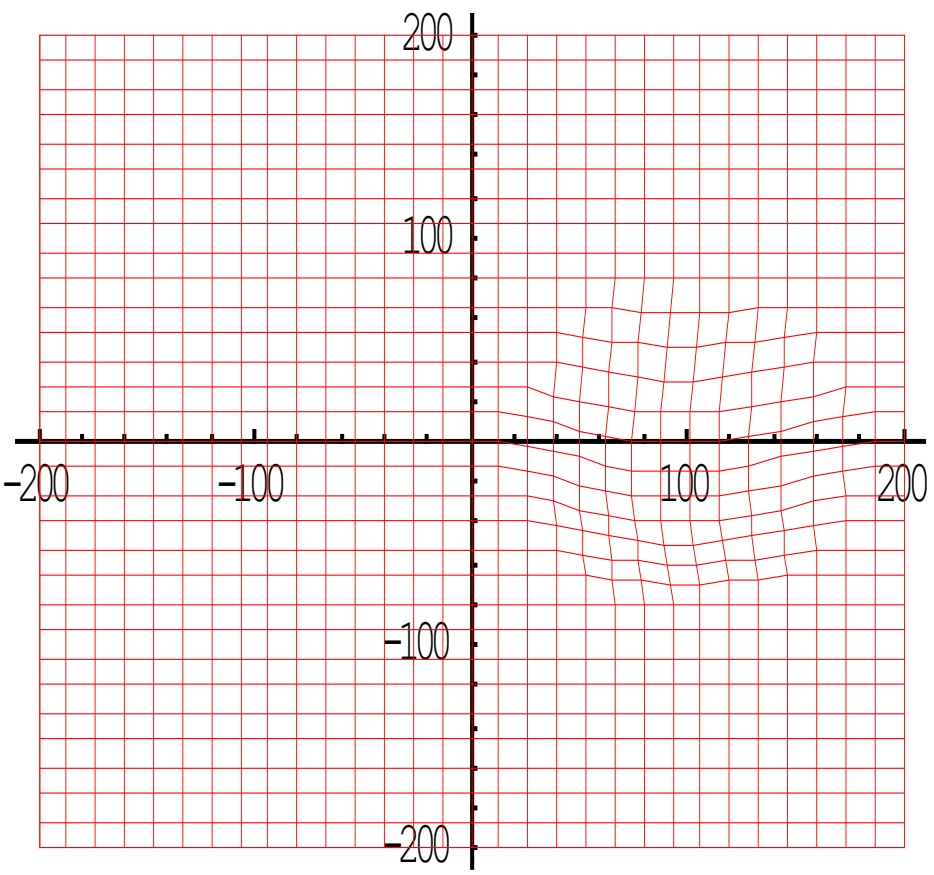

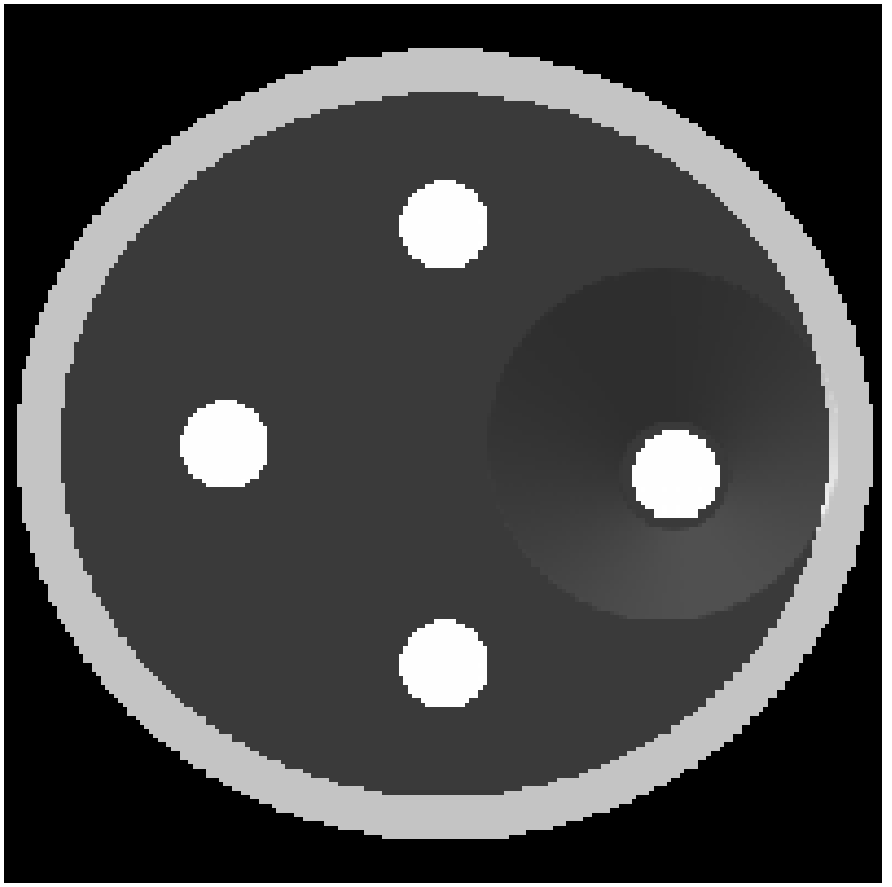

Original image of the phantom at an intermediate time.

Numerical experiment

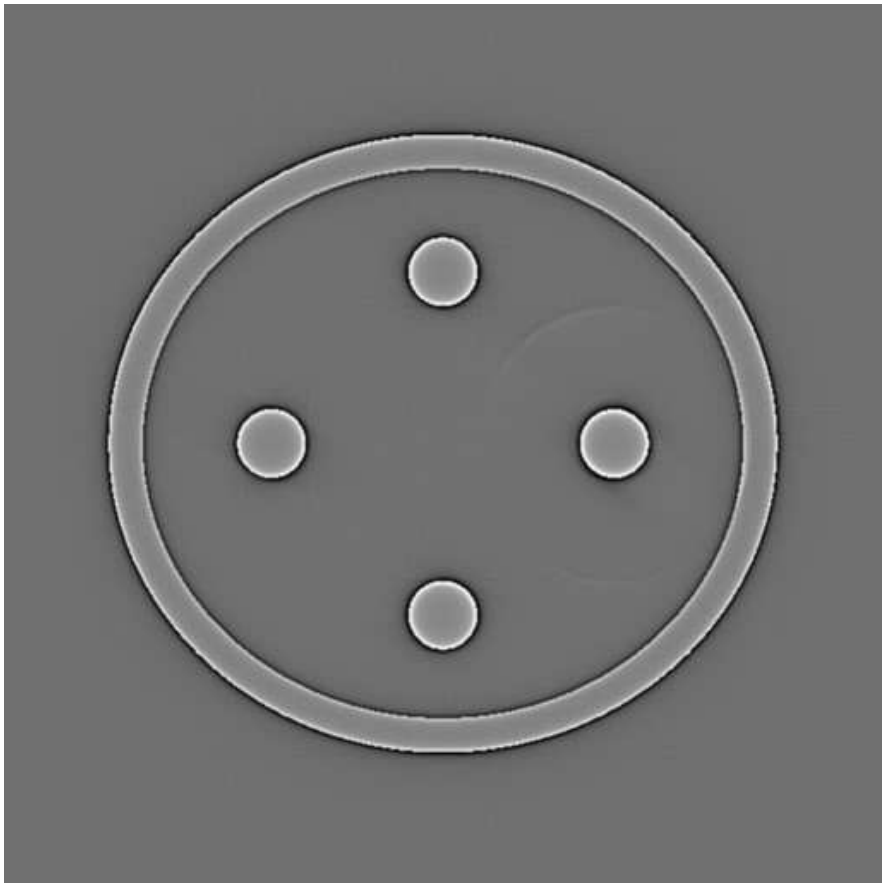

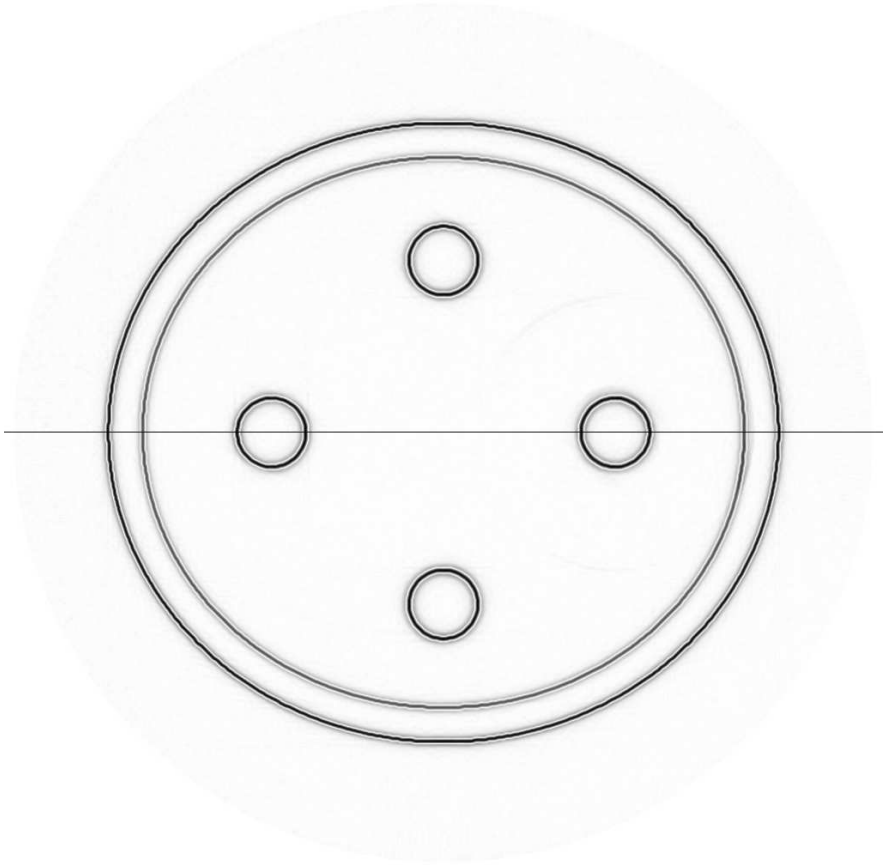

Left panel - LT function f_Λ, right panel - gradient of f_Λ.

Numerical experiment

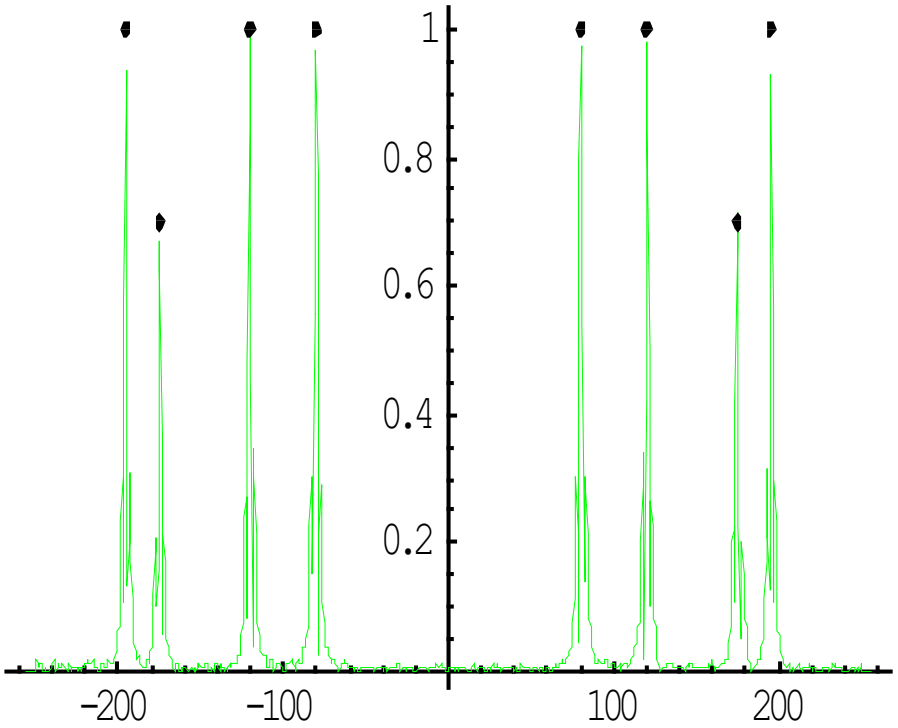

Cross-section through the normalized gradient of the f_Λ along the line shown in the previous slide.

Experiment with noise

Poisson noise was added to the projection data. It was computed based on 10^4 incident photons per detector element. All other simulation/reconstruction parameters are the same.

Experiment with noise

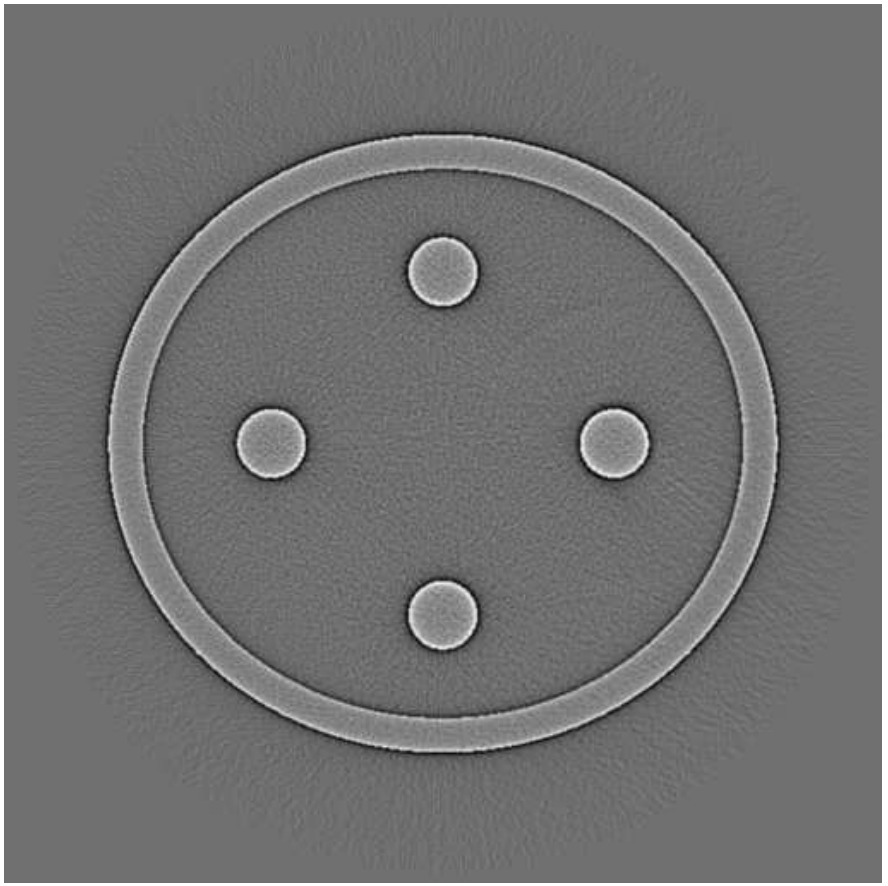

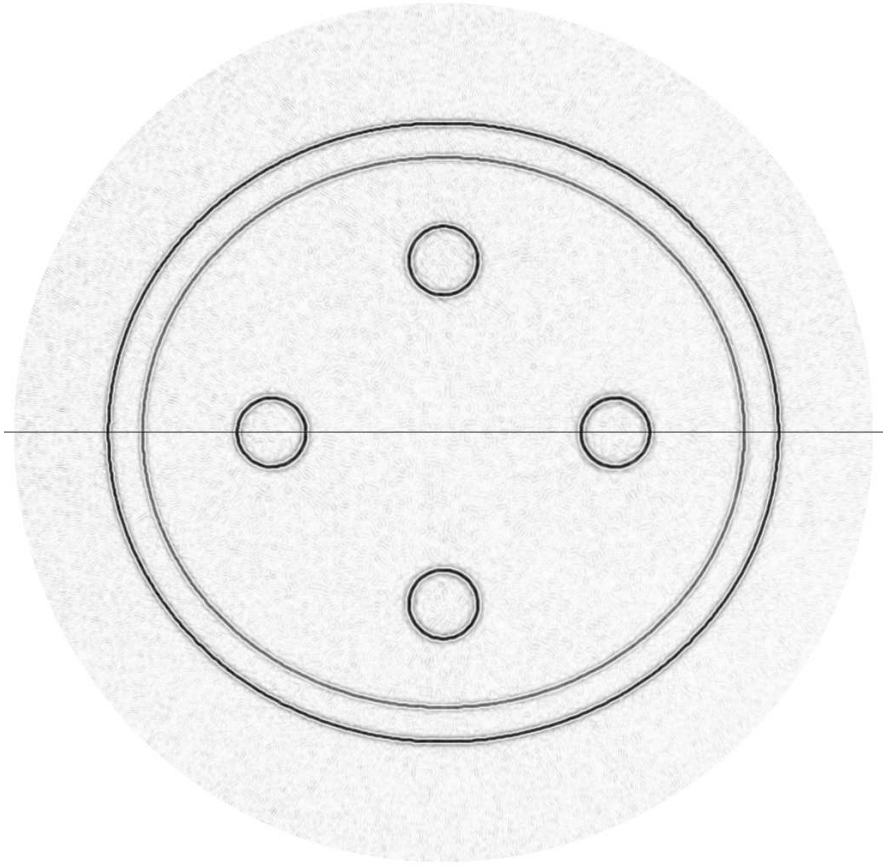

Left panel - LT function f_Λ, right panel - gradient of f_Λ.

Experiment with noise

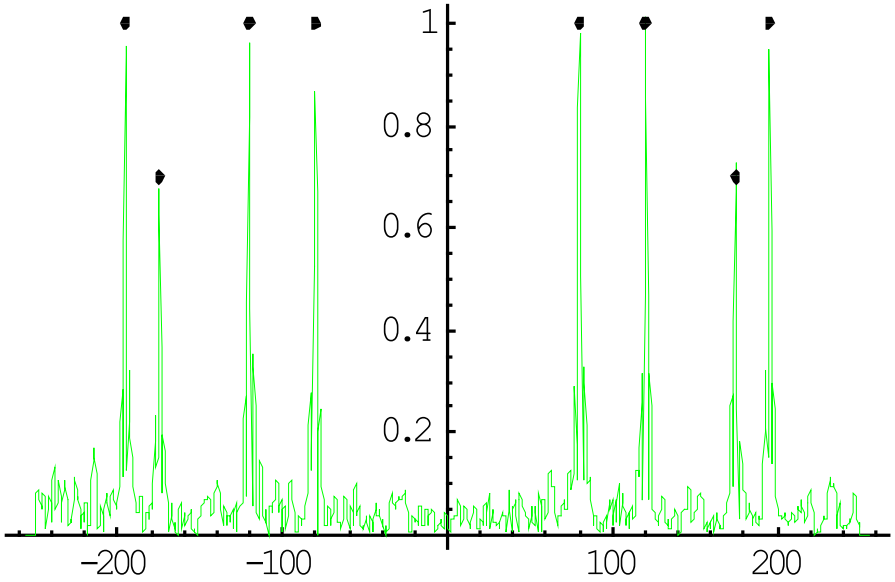

Cross-section through the normalized gradient of the f_Λ along the line shown in the previous slide.

Frequency-split reconstruction

Recall that if

$$f_{pl}(x) = \frac{1}{2\pi}|x|_{\epsilon}^{-1} * f_{\Lambda}(x).$$

then $f - f_{pl}$ is smoother than f in the scale of Sobolev spaces.

Frequency-split reconstruction

Evaluating the integral and keeping the leading singular terms gives

$$f_{pl}(x) \sim \frac{R}{2\pi^2} \int_0^T \Psi(s,x) \int \frac{g'_u(s,u)}{u_x - u} du ds.$$

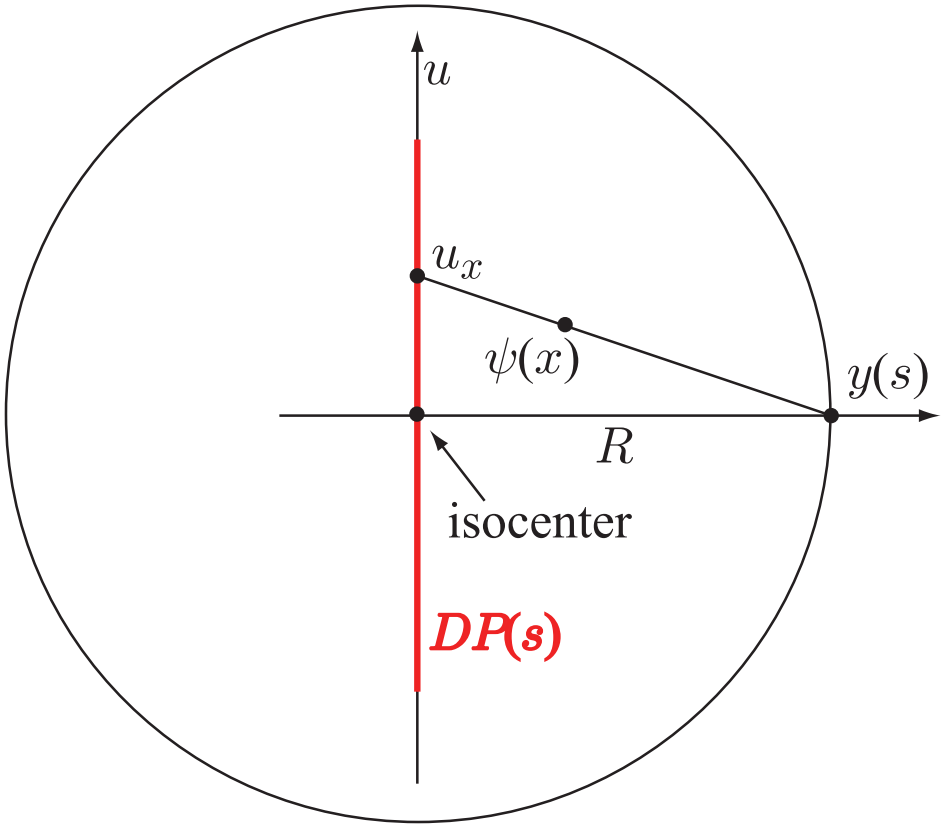

Frequency-split reconstruction

$$\Psi(s,x) = \frac{\varphi(s)\kappa(\theta'(s,x))}{\bar{\varphi}(x,\theta(s,x))} \frac{|A'_s \cdot \Theta|}{|\nabla\mu(s,\psi(s,x))\beta(s,x)|} \times \frac{|[\nabla\psi(s,x)]^t\Theta|^2}{|\psi(s,x)-y(s)|^2(e^{\perp}\cdot\Theta)^2}.$$

After f_{pl} is found, the difference $f - f_{pl}$ can be computed iteratively.

Numerical experiments

We use the same motion model and phantom as in the case of local tomography.

Numerical experiments

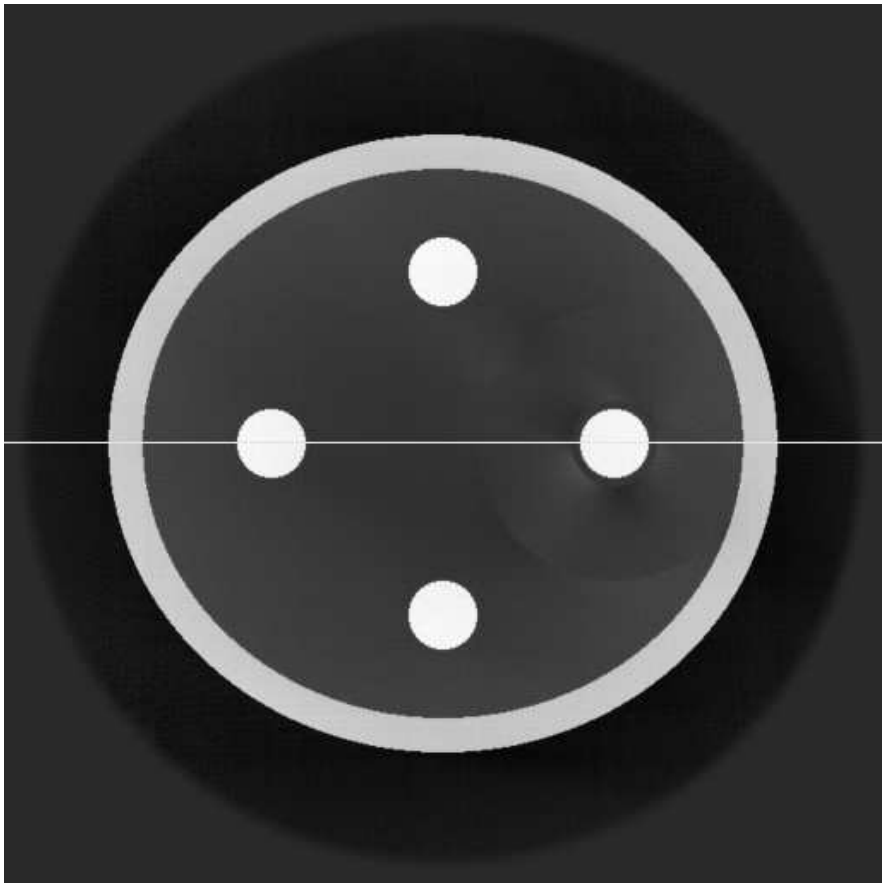

High-frequency localized reconstruction at reference time. Full grey level scale. Noise-free data, correct motion model.

Numerical experiments

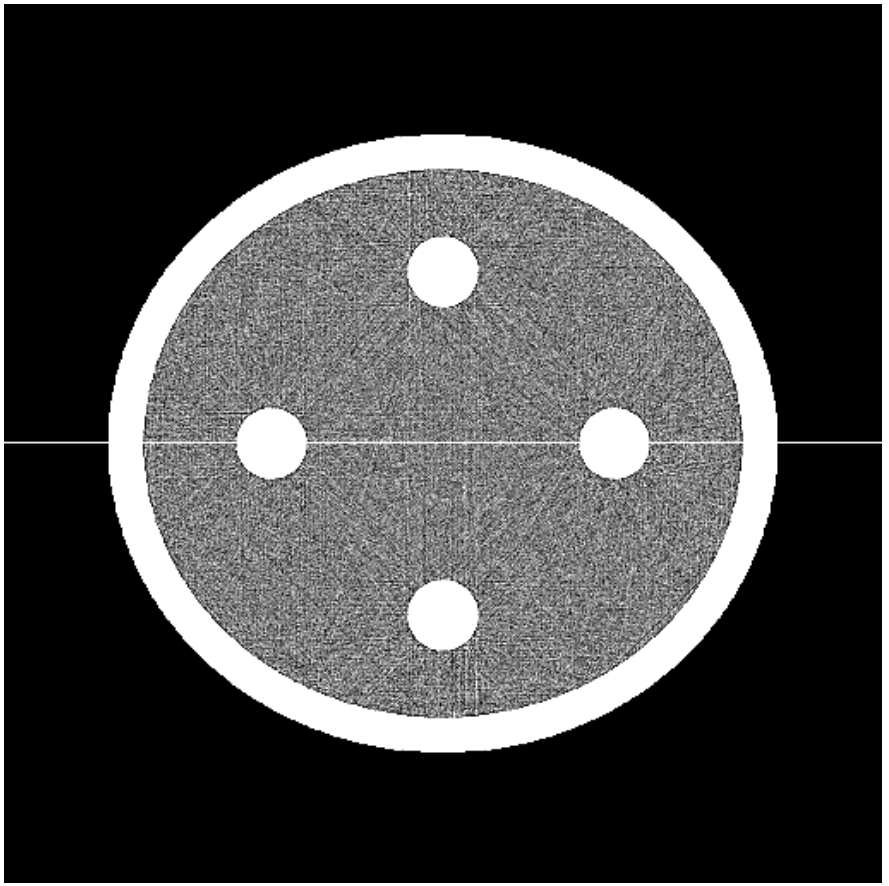

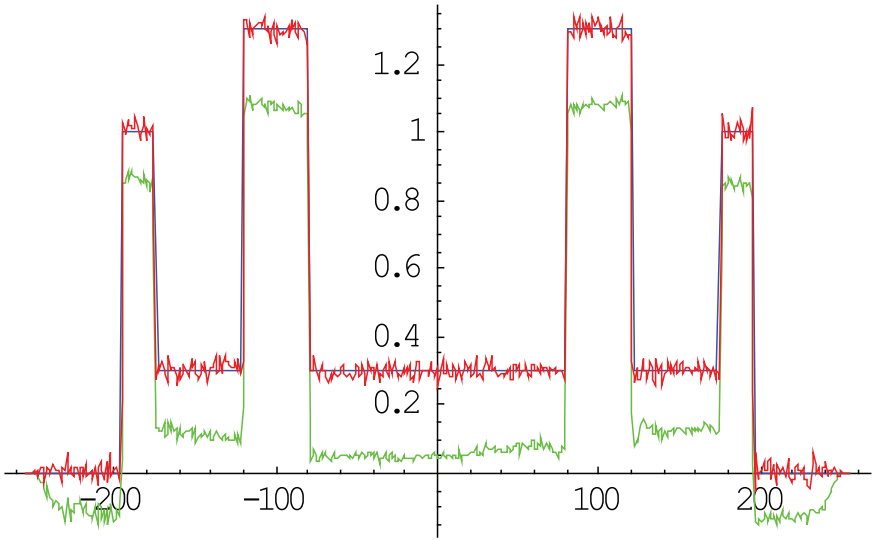

Hybrid reconstruction. Noise-free data, correct motion model. Compressed grey level scale.

Numerical experiments

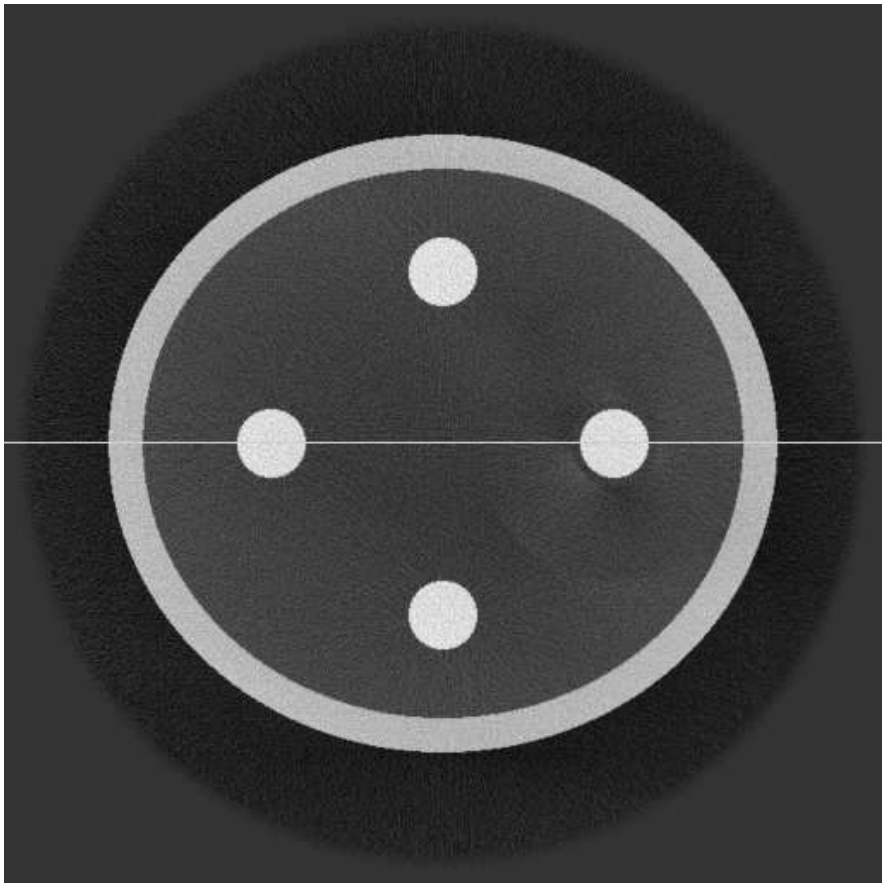

High-frequency localized reconstruction at reference time. Full grey level scale. Noisy data, correct motion model.

Numerical experiments

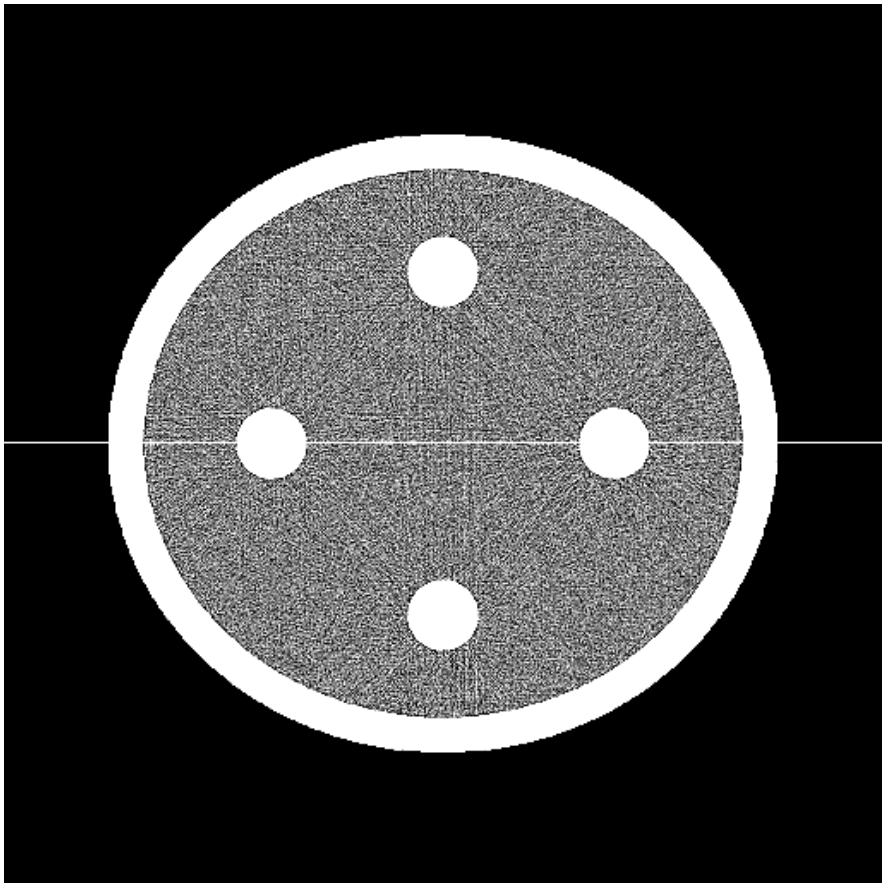

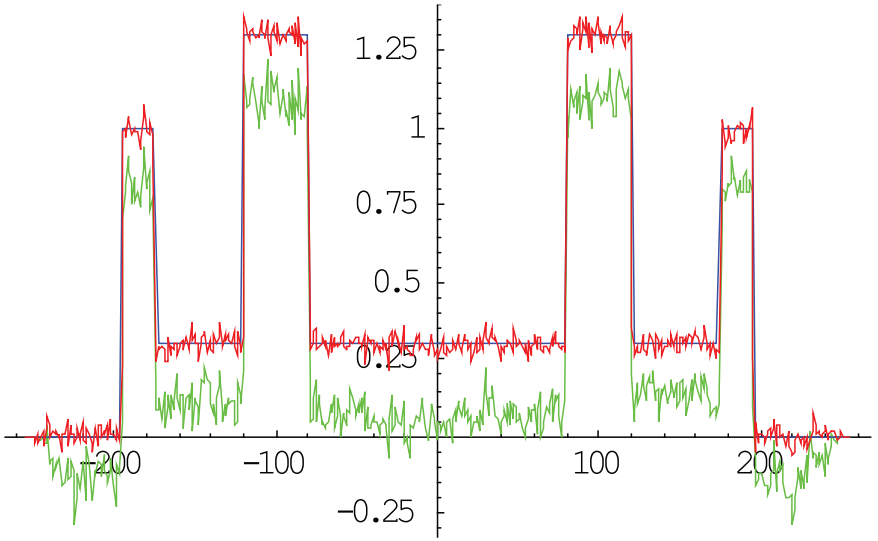

Hybrid reconstruction. Noisy data, correct motion model. Compressed grey level scale.

Numerical experiments

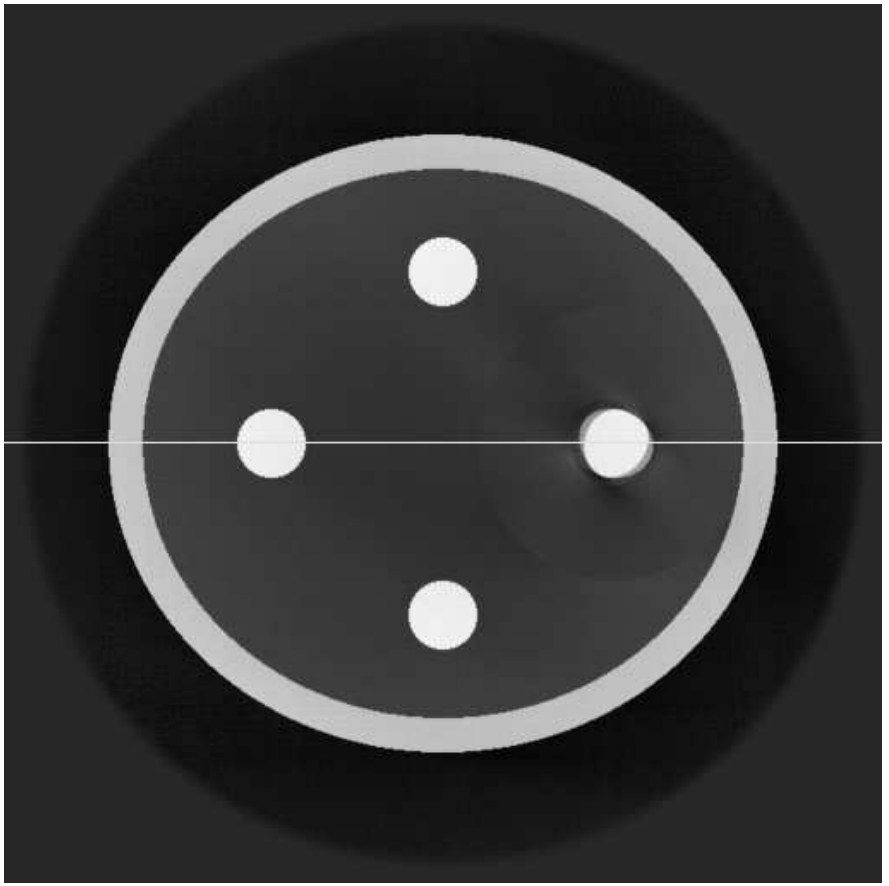

High-frequency localized reconstruction at reference time. Full grey level scale. Noise-free data, wrong motion model.

Numerical experiments

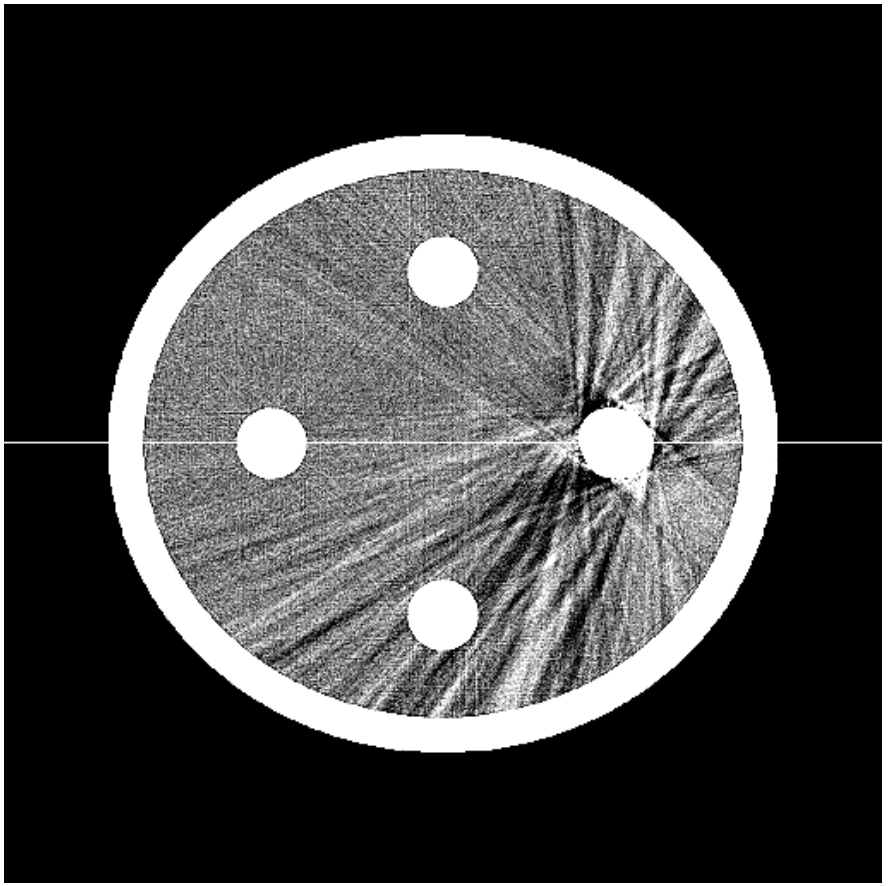

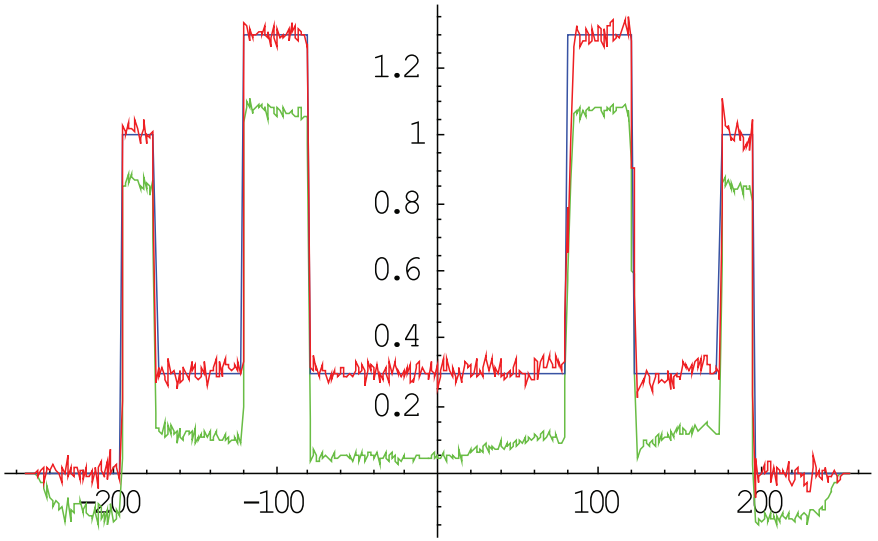

Hybrid reconstruction. Noise-free data, wrong motion model. Compressed grey level scale.

Numerical experiments

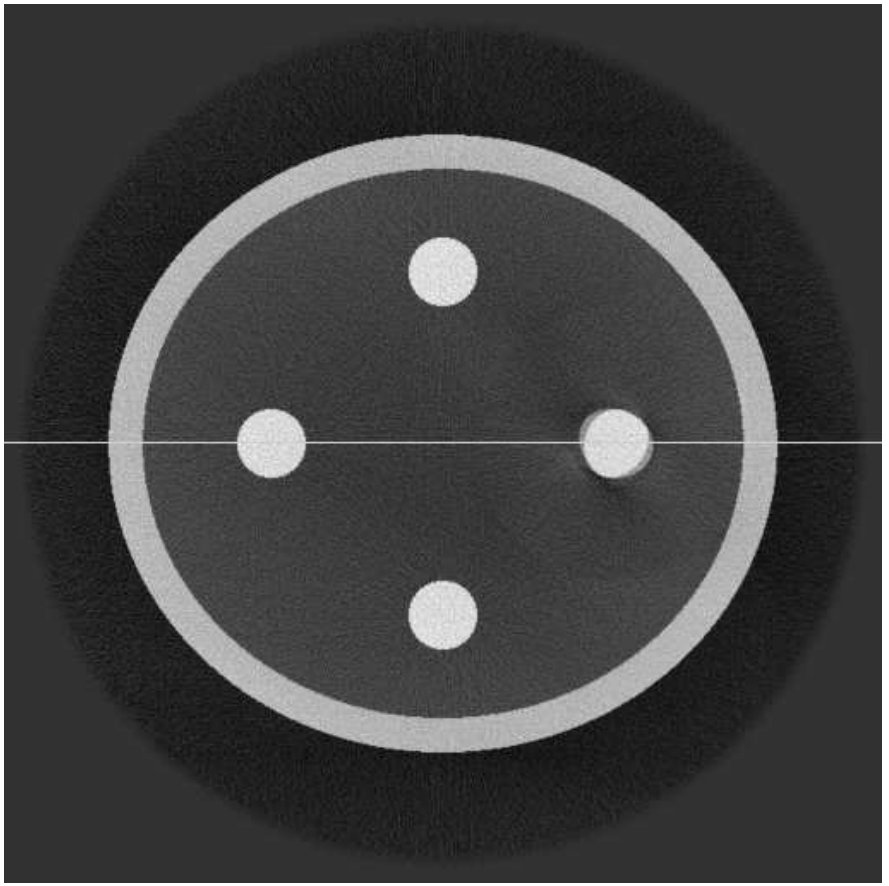

High-frequency localized reconstruction at reference time. Full grey level scale. Noisy data, wrong motion model.

Numerical experiments

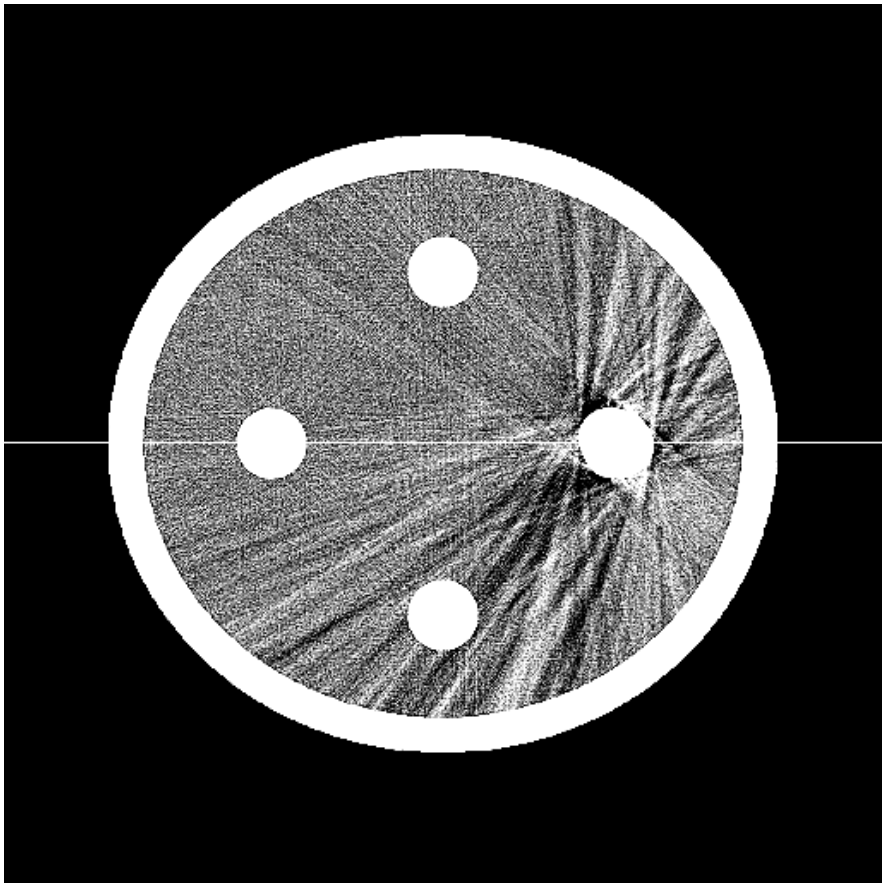

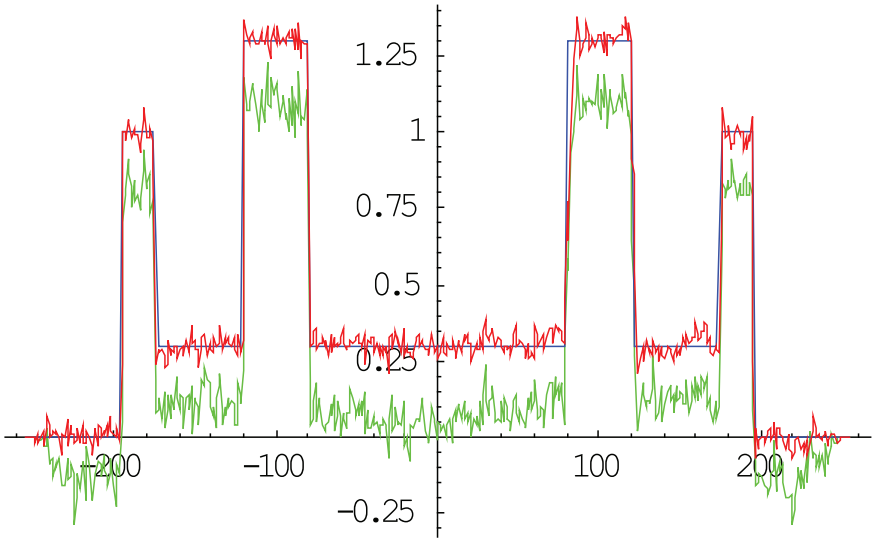

Hybrid reconstruction. Noisy data, wrong motion model. Compressed grey level scale.